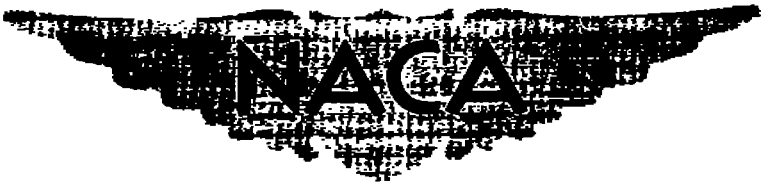

RESEARCH MEMORANDUM

CALCULATED REACTIVITY OF URANYL-FLUORIDE - WATER CRITICALITY EXPERIMENTS

By Donald Bogart and Leonard Soffer

Lewis Flight Propulsion Laboratory
Cleveland, Ohio

NATIONAL ADVISORY COMMITTEE
FOR AERONAUTICS

WASHINGTON
March 30, 1956
Declassified October 28, 1960

NACA RM E55L23

NATIONAL ADVISORY COMMITTEE FOR AERONAUTICS

RESEARCH MEMORANDUM

CALCULATED REACTIVITY OF URANYL-FLUORIDE - WATER CRITICALITY EXPERIMENTS

By Donald Bogart and Leonard Soffer

SUMMARY

A modified group method has been used to calculate the reactivity of the uranyl-fluoride - water experimental critical assemblies which are part of the Oak Ridge critical mass studies. The method employed relates the experimental slowing-down length for water to that in fluoride solutions and includes the effects of epithermal absorption and fission. The reactivity was calculated for 35 bare and 85 water-reflected experimental critical configurations. These configurations covered a wide range of uranium concentrations and core geometries. Calculated reactivities were reasonably good for all the reflected assemblies and for all bare assemblies except those having the highest uranium concentrations.

INTRODUCTION

Reactor design groups generally require criticality calculations of a survey type in which many kinds of reactors are parametrically investigated. For such work two- or three-group analysis has been found most useful. Furthermore, desirable design information regarding effects of nonuniform spatial distributions of fuel and absorbers, two- or three-dimensional flux distributions, and effects of local inhomogeneities on flux and reactivity is more readily obtained within the limits of diffusion theory from two- or three-group analysis. For example, a two-group formulation which includes the effect of epithermal processes was used in the following studies at the NACA Lewis laboratory:

(1) Criticality surveys of enriched-uranium hydroxide-moderated reactors of interest in aircraft nuclear propulsion (refs. 1 and 2)

(2) Achievement of flat spatial power generation by nonuniform distribution of uranium in water-moderated reactors (ref. 3)

(3) Spatial burn-out of fuel and burnable poison in water reactors designed for increased reactor life (ref. 4)

(4) Calculation of neutron fluxes in the vicinity of control rods (ref. 5)

For water-moderated reactors with significant neutron production at epithermal energies, a modified group method was formulated which considers the details of the processes in the epithermal region (ref. 6).

The validity of reactor criticality calculations by group methods is best tested by applying these methods to a set of controlled critical experiments. The Oak Ridge critical mass studies (refs. 7 and 8) provide an excellent set of experiments to check diffusion-theory group analysis as it applies to hydrogen-moderated reactors. These experiments are ideal for analysis, as they consist of homogeneous solutions of uranyl fluoride in water enclosed by thin aluminum or stainless-steel cylindrical containers with and without water reflectors. The uranium is enriched to contain 93.4 percent uranium-235. The modified group method of reference 6 is applied herein to all the bare and water-reflected critical experiments reported in reference 7, with the exception of the cadmium-covered water-reflected cases. In addition, the results of an extended program of critical experiments in cylindrical geometry reported in reference 8 are included in the present analysis. The group formulation employed makes use of the peculiarly rapid slowing-down properties of hydrogen and includes the effects of epithermal absorption and fission. The concept of reflector savings, calculated by two-group analysis, is employed in evaluating the criticality of the reflected experimental assemblies.

Since the experiments of reference 7 were reported, these data have been widely analyzed. Schuske and Morfitt (refs. 9 and 10) in seeking safe handling procedures succeeded in fitting the experimental data to empirical curves. Macklin (ref. 11) later improved the empirical relations in order to extend the data beyond the experimental range. Clark (ref. 12) applied a one-group neutron diffusion model to the experimental data in order to establish a basis for estimating the nuclear safety of separation-process equipment.

Various investigators, led by Greuling (refs. 13 and 14), have attempted to obtain a comprehensive yet simple theory of the hydrogen-moderated reactor. Mills, Bell, Bendt, and Danzker (refs. 15, 16, 17, and 18, respectively) have analyzed the experimental data with such an object in mind. With individually varying methods, all have obtained

reasonable results. The present report attempts to determine how the modified group method of criticality analysis, employed in NACA analytical reactor studies, predicts the reactivity of the water reactors of references 7 and 8.

ANALYSIS

The group diffusion method used includes the effects of epithermal absorption and fission and employs the following facts for neutrons slowing down in hydrogenous media:

(1) The bulk of the contribution to the mean-square slowing-down length to thermal energies L_f^2 takes place above the epithermal region.

(2) Epithermal absorption occurs near thermal energy, mostly in the energy range below about 1000 electron volts.

If age theory is taken to apply in the epithermal region, the slowing-down, diffusion, and absorption processes in this region may be treated in detail. To accomplish this, neutrons are divided into three separate regions: fast, epithermal, and thermal. All neutron absorption, and therefore production, is restricted to the epithermal and thermal regions. Group-diffusion slowing down in the fast region and Fermi-age slowing down in the epithermal region are assumed.

If $L_i^2(E)$ is defined as the mean-square slowing-down length for neutrons of fission energies to energy E, and $\tau_i(E)$ is the Fermi age for neutrons from E_{th} to E (where E is any energy in the epithermal region; i.e., $E_i \geq E \geq E_{th}$), then $L_i^2(E)$ and $\tau_i(E)$ are given by

$$L_i^2(E) = L_f^2 - \tau_i(E)$$

$$\tau_i(E) = \int_{E_{th}}^{E} \frac{1}{3\xi \Sigma_{TR} \Sigma_T} \frac{dE}{E}$$

where Σ_{TR} and Σ_T are energy-dependent macroscopic transport and total cross sections, respectively, and ξ is the average loss in log

energy per collison. This three-energy-region picture leads to the following criticality equation (see appendix A for definition of symbols):

$$\frac{K_{th}p_{th}}{\left(1 + L_f^2B^2\right)\left(1 + L_{th}^2B^2\right)} + \int_{E_{th}}^{E_1} \frac{K_1(E)\,\frac{dq(E)}{d(E)}\,dE}{1 + \left[L_f^2 - \tau_1(E)\right]B^2} = K_{eff} \qquad (1)$$

The first term represents the contribution to the neutron generation due to fissions by thermalized neutrons, wherein the quantity $1/\left(1 + L_f^2B^2\right)$ is the probability of a neutron escaping leakage in slowing down to thermal energies in a medium of buckling constant B^2; p_{th} is the fraction of fission neutrons absorbed that escape capture in slowing down to thermal energies; $1/\left(1 + L_{th}^2B^2\right)$ is the probability of a neutron escaping leakage during thermal diffusion; and K_{th} is the thermal multiplication constant.

The integral term represents the contribution to the neutron generation due to epithermal fission. In this integral, the quantity $1/\left\{1 + \left[L_f^2 - \tau_1(E)\right]B^2\right\}$ represents the nonleakage probability for a neutron slowing down from fission energies to some epithermal energy E; $\frac{dq(E)}{d(E)}\,dE$ represents the fraction of the total fission neutrons absorbed that are captured in the epithermal-energy interval dE and is the change in slowing-down density $q(E)$ across the interval dE; and, finally, $K_1(E)$ is the epithermal multiplication constant at energy E given by $\nu\Sigma_F(E)/\Sigma_A(E)$, where Σ_F and Σ_A are local values of macroscopic fission and absorption cross sections for the medium.

Evaluation of this integral term permits a detailed determination of the disposition of neutrons by leakage, absorption, and slowing within the epithermal region. However, it is possible and desirable to replace the integral term by a more convenient term involving quantities averaged over the epithermal region. The average values are obtained by weighting local values by the neutron fluxes in this epithermal region. The variation of neutron flux with energy is evaluated on the basis of an appropriate neutron slowing-down model in an infinite medium of the same composition. In the present analysis the age-theory model has been used, since, for the reactors under consideration, the important nonthermal contributions occur in the epithermal region where

age theory is a good approximation. In this manner average values of epithermal multiplication constant $\overline{K}_1$ and average epithermal age $\overline{\tau}_1$ are numerically determined (see appendix B).

The integral $\int_{E_{th}}^{E_1} \frac{dq(E)}{d(E)}\, dE$ is simply $\left[q(E_1) - q(E_{th})\right] = (1 - p_{th})$.

Inasmuch as there are no absorptions at energies above E_1, $q(E_1) = 1$, and by definition $q(E_{th}) = p_{th}$.

The average mean-square slowing-down length for fission neutrons to the epithermal region is then given by $\left(L_f^2 - \overline{\tau}_1\right)$, and the probability of a fission neutron escaping leakage in slowing through the epithermal region is given by $1/\left[1 + \left(L_f^2 - \overline{\tau}_1\right)B^2\right]$. This term takes cognizance of the effectively reduced slowing-down distance for epithermal neutrons resulting from absorption of such neutrons and its effect on neutron leakage in the epithermal region.

With these simplifications, the criticality equation (1) now becomes

$$\frac{K_{th}p_{th}}{\left(1 + L_f^2B^2\right)\left(1 + L_{th}^2B^2\right)} + \frac{\overline{K}_1(1 - p_{th})}{1 + \left(L_f^2 - \overline{\tau}_1\right)B^2} = K_{eff} \qquad (2)$$

It is this equation which has been applied to the criticality data of references 7 and 8. The specific procedures for evaluating the required parameters and values for these parameters are presented in appendix B.

Briefly, parameters K_{th} and L_{th}^2 are calculated from their definitions; that is, $K_{th} = \nu\Sigma_{F,th}/\Sigma_{A,th}$ and $L_{th}^2 = \lambda_{TR,th}/3\Sigma_{A,th}$ (effect of chemical binding of hydrogen in the water molecule on $\lambda_{TR,th}$ is approximated). An average epithermal multiplication constant $\overline{K}_1$ may be evaluated by numerical integration for a given core composition by age theory. It has been shown in reference 2 that $\overline{K}_1$ may be correlated with the value of K_{th} for a given core composition, inasmuch as uranium is the only absorber whose cross section does not vary inversely with neutron velocity. The correlation of K_{th} and $\overline{K}_1$ for a wide range of reactor core compositions is given in reference 2 and is used herein.

The quantity L_f^2 has been calculated for water and UO_2F_2-H_2O solutions by the method of Marshak and averaged over the fission spectrum. These calculated results are normalized to the experimental value of L_f^2 of 31.8 square centimeters for pure water and presented as a function of the hydrogen to uranium-235 atom ratio R (see appendix B).

The geometric bucklings B^2 used were computed by use of an extrapolation distance based on properties of the fast-neutron group (1-Mev region) for bare reactors or based on calculated two-group reflector savings for spherical reflected reactors of the same composition.

RESULTS AND DISCUSSION

The results of the criticality calculations for the bare and water-reflected cylindrical-reactor experiments of references 7 and 8 are presented in figures 1 and 2, respectively. The effective multiplication constant K_{eff} as calculated from equation (2) is plotted against the H/U-235 atom ratio R. A distinction is made between the aluminum- and steel-enclosed reactors of various diameters. In references 7 and 8, for reactors of a given diameter, the core height was varied to obtain criticality for solutions of different uranium concentration corresponding to the ordinate R. The material parameters used in computing values of K_{eff} for all values of R are given in table I.

The results for the bare reactors shown in figure 1 indicate an approximate average K_{eff} of 0.98 with a scatter of ΔK of about ± 0.01 for values of R above 100. With uranium enrichment to values of R below about 100, the reactors are gradually predicted to be more subcritical. For reactors with R of 25, some 80 percent of the fissions occur epithermally; whereas, for R of 100, but 35 percent of the fissions occur epithermally.

It is recalled that the average energy of the leakage neutrons has been considered to be about 1 Mev, and cross sections at this energy have been used to evaluate the extrapolation distance δ. It will be shown later that calculated values of K_{eff} are quite sensitive to δ. By using larger values of δ corresponding to cross sections at energies slightly higher than 1 Mev, calculated values of K_{eff} are increased. Therefore, the lower predicted values of K_{eff} for the more epithermal critical assemblies (low R) shown in figure 1 may be due to leakage neutron spectrums of average energy greater than 1 Mev.

The results for the water-reflected reactors are shown in figure 2. There is apparently a much greater scatter than for the bare reactors; however, two important things are noted:

(1) The aluminum- and steel-container points are separated some 0.02 to 0.03 in ΔK. Within each group of points the scatter is about ± 0.01 about an average value of K_{eff} of 0.98 for the aluminum-contained assemblies and about an average value of K_{eff} of 1.00+ for the steel-contained assemblies.

3602

(2) The tendency for the richer reactors to be predicted more subcritical is not present for the aluminum-contained assemblies, but this trend exists for the steel-contained assemblies below values of R of about 50. For the lower values of R, both aluminum and steel points run together.

The separation of the aluminum and steel points may be explained by the following: In computing K_{eff} for the reflected reactors, no distinction is made between the aluminum and steel reactor containers. It was assumed that a thin metal shell would have negligible reflector effectiveness compared with a thick water reflector. Although this may be quite true, the cross sections for iron and aluminum are markedly different for fast and thermal neutrons. The fast-scattering cross sections for iron and aluminum are both of the order of 3 barns, but the thermal-absorption cross section for iron is more than 10 times that of aluminum (2.43 barns compared with 0.21 barn).

The effectiveness of the water reflector, therefore, would be expected to be relatively unchanged by the container for highly epithermal reactors that do not rely significantly on reflected thermalized neutrons. On the other hand, for more thermal reactors, the steel container intercepts a larger fraction of the reflected thermalized neutrons than the aluminum container. Thus, the reactivity computed for highly epithermal aluminum- and steel-contained reactors (lower values of R) are practically identical, as indicated in figure 2. For larger more thermal reactors (higher values of R), the steel shell absorbs more of the thermal neutrons returned to it by the reflector than the aluminum shell, and the predicted K_{eff} values diverge from each other. The steel-contained reactors are calculated to be more supercritical than the aluminum-contained reactors, because the relative absorption of the shells has not been taken into account.

In appendix C, the effects upon K_{eff} of the estimated experimental error cited by the authors of reference 7 in measuring critical core height and uranium concentration of the water-fluoride mixtures are evaluated for representative core configurations. Summarizing briefly, the

uncertainty in the critical height measurement may introduce a variation in K_{eff} of 0.7 percent for the flatter reactors, whereas the uncertainty in uranium concentration may introduce a variation in K_{eff} of 0.6 percent for the leaner reactors. The experimental errors may therefore account for much of the scatter in the data.

The tendency for the richer reactors (smaller R) to be calculated as less reactive than the leaner reactors (larger R) has also been found by Mills (ref. 15). By use of the Goertzel-Selengut method applied to the ANP multigroup technique he calculated K_{eff} for four of these configurations, two bare and two reflected. In the following table Mill's results are compared with those obtained in this report:

Diameter, cm	Height, cm	Container material	Reflector thickness, cm	Critical mass, Kg U-235	Atom ratio, R	K_{eff}	
						Ref. 15	Present report
25.4	34.0	Al	0	7.9	52.9	1.005	0.979
25.4	32.3	Steel	0	8.8	43.9	.981	.967
38.1	44.3	Al	11.43	1.31	999	1.008	.972
25.4	22.4	Al	19.78	.893	329	1.007	.978

Both methods are in relative agreement in predicting the reactivity of the bare reactors, and both show the same trend in underestimating K_{eff} for the richer of the two bare reactors. For the two reflected cases, Mills estimates reactivity as about 1 percent supercritical, and the present report estimates these as about 2 percent subcritical. However, the indications are that use of two-group reflector savings, which were calculated for reactors of spherical geometry and applied herein to the experimental assemblies, is satisfactory. The following discussion will indicate that the consistently subcritical predicted reactivities for bare assemblies may be explained by considerations of the extrapolation length.

The extrapolation length δ, whose calculation is described in appendix B, is an important quantity used in computing the geometric buckling for bare reactors. The quantity δ was arbitrarily computed from the transport mean free path evaluated from cross sections at a neutron energy of about 1 Mev. This assumed that 1 Mev was representative of the energy of the leakage neutrons. It is quite possible that a somewhat higher energy should be used with corresponding smaller cross sections, leading to a slightly larger extrapolation length.

In order to determine the effect on the predicted reactivity of a change in the extrapolation length δ, the criticality of all the bare reactors was recomputed with values of δ increased by 10 percent over

those used for figure 1 (these appear in table I). The results of these calculations are shown in figure 3. Comparison of figures 1 and 3 indicates that arbitrarily increasing the extrapolation distance serves to shift the data in a more or less uniform way, making the reactivity predictions closer to unity. The flatter reactors (larger diameters) as a group are more sensitive to changes in δ. Since they are flat, the axial buckling is sensitive to changes in the extrapolation length. It is apparent that no one value of δ can serve for all the data points.

Clark (ref. 12) has used the Oak Ridge critical mass study data to calculate extrapolation distances; and his results, which vary from 3.0 to 3.5 centimeters, agree with the values used herein. The indications are that the choice of 1 Mev as a neutron energy to select cross sections for estimating values of δ is satisfactory for hydrogen-moderated critical assemblies.

CONCLUSIONS

A modified group method of criticality analysis, employed in various NACA analytical reactor studies, was applied to the experimental configurations which are part of the Oak Ridge critical mass studies. The calculated reactivities of these uranyl-fluoride - water critical assemblies were reasonably good for all the reflected and most of the bare cores over the entire range of uranium concentration and core geometry covered by the Oak Ridge experiments. The effects of aluminum and steel containers on the reactivity of water-reflected assemblies were indicated.

Lewis Flight Propulsion Laboratory
National Advisory Committee for Aeronautics
Cleveland, Ohio, December 31, 1955

APPENDIX A

SYMBOLS

The following symbols are used in this report:

B^2	geometric buckling constant
E	neutron energy
K	neutron multiplication constant
K_{eff}	effective multiplication factor
L^2	mean-square slowing-down length, cm^2
N	reactor atom density
N_0	Avogadro's number (6.023×10^{23} atoms/mole)
p_{th}	fraction of fission neutrons escaping capture in slowing
q	slowing-down density
R	atom ratio of hydrogen to U-235
t	reflector thickness, cm
δ	extrapolation length or reflector savings, cm
λ	neutron mean free path
ν	number of neutrons produced per fission
ξ	average loss in log energy per neutron collision
ρ	density
Σ	macroscopic cross section
σ	microscopic cross section
τ	Fermi age, cm^2

Subscripts:

A	absorption
C	core
F	fission
f	fast-neutron group
i	intermediate neutron group
r	reflector
S	scattering
T	total
TR	transport
th	thermal neutron group

APPENDIX B

EVALUATION OF CRITICALITY PARAMETERS

In the criticality equation used to calculate K_{eff} (eq. (2)), the required parameters fall into the following categories:

Thermal: Thermal multiplication constant, K_{th}; thermal diffusion length, L^2_{th}.

Epithermal: Epithermal multiplication constant, $\overline{K}_1$; average epithermal Fermi age, $\overline{\tau}_1$; noncapture probability, p_{th}.

Fast: Mean-square slowing-down length, L^2_f.

Geometric buckling constant: B^2.

Thermal Parameters

The thermal parameters are calculated from their definitions as follows:

$$K_{th} = \frac{\nu \Sigma_{F,th}}{\Sigma_{A,th}}$$

$$L^2_{th} = \frac{\lambda_{TR,th}}{3\Sigma_{A,th}}$$

where $\Sigma_{A,th}$ is the macroscopic thermal absorption, and $\Sigma_{F,th}$ is the macroscopic fission cross section. Both cross sections are averaged over the Maxwellian distribution of thermal neutron flux. The neutron yield per fission ν has a value of 2.46, and $\lambda_{TR,th}$ is the thermal-transport mean free path. The value of the hydrogen-transport cross section is affected by the chemical binding of the hydrogen atom to the water molecule. Radkowsky's method of computing the thermal-transport microscopic cross section for hydrogen was used in reference 2; a value of 31.4 barns at room temperature was obtained and is used here.

The hydrogen atom concentration N^H must be known to evaluate these constants. The criticality data in reference 7 gave the U-235

density and the N^H/N^{U-235} ratio for many solutions; N^H, therefore, was computed as a function of N^H/N^{U-235}, as follows:

$$N^H = \frac{N^H}{N^{U-235}} \frac{\rho N_0}{235}$$

where ρ = g U-235/cc of solution, and N_0 = Avogadro's number. These data are presented in figure 4 and do not fall on a smooth curve (the authors estimate a ±2-percent error in determination of ρ). A smooth curve was accordingly drawn through these points and required values of N^H were read from figure 4. This curve shows how the hydrogen atom concentration is decreased substantially for the rich solutions and approaches the value for pure water (0.0668×10^{24} atoms/cc) as the solutions become leaner.

3602

In the following table are listed the microscopic cross sections of the elements hydrogen, oxygen, U-235, and fluorine for absorption and scattering at 0.025 electron volt and an average fast-scattering cross section at about 1 Mev. These values were obtained from references 19 and 20 and their respective supplements:

Element	σ_A(0.025 ev)	σ_S(0.025 ev)	$\bar{\sigma}_S$(1 Mev)
H	0.33	[a]31.4 ($\bar{\sigma}_{TR}$)	4.5
O	0	4.18	3.5
U-235	687 580 (σ_F 0.025)	10.0	7.0
F	0	3.94	3.0

[a]Average over Maxwellian thermal neutron flux distribution considering chemical binding (ref. 2).

Epithermal Parameters

As mentioned previously, the required average epithermal parameters are obtained by numerically weighting values at various energies by corresponding neutron fluxes. The variation of neutron flux with energy is taken as that for the neutron slowing-down distribution according to age theory in an infinite medium of the same composition. Values of $\bar{K}_1$ and p_{th} have been evaluated in this way (see ref. 1). References 2 and 6 show that values of $\bar{K}_1$, numerically determined for many core compositions, may be correlated with K_{th} for reactors where there is

significant epithermal production. Such a correlation, valid for hydrogenous reactors, is given in references 2 and 6 and is used herein to evaluate $\overline{K}_1$. Bendt (ref. 17) has also used this correlation.

The quantity $\left(L_f^2 - \overline{\tau}_1\right)$ represents an average slowing-down length for neutrons of intermediate energy. Therefore, $1/\left[1 + \left(L_f^2 - \overline{\tau}_1\right)B^2\right]$ represents the probability that a neutron will not leak out of the reactor while slowing down from fission energies through epithermal energies. In a reactor having considerable epithermal absorption and production, this factor can be of importance. This quantity was computed by first evaluating $\tau(E)$ from the Fermi age equation given before; $\tau(E)$ was then weighted by the slowing-down density from the age-theory model, and an average $\overline{\tau}_1$ was calculated as follows:

$$\overline{\tau}_1 = \frac{\int_{E_{th}}^{E_1} \tau_1(E)\,\frac{dq(E)}{dE}\,dE}{\int_{E_{th}}^{E_1} \frac{dq(E)}{dE}\,dE}$$

Values of $\overline{\tau}_1$ varied from 0.20 square centimeter for lean solutions to 1.5 square centimeters for the richer solutions; $\overline{\tau}_1$ is presented as a function of R later in figure 6.

The noncapture probability for neutrons slowing down in infinite hydrogenous moderators containing heavy absorbers is given by equation 6.88.1 in Glasstone and Edlund (ref. 21) as

$$p_{th} = \exp\left[-\int_{E_{th}}^{E_0} \frac{\Sigma_A dE}{(\Sigma_A + \Sigma_S)E}\right]$$

If it is assumed that hydrogen is the only scatterer and that other absorbers obey the 1/v law in the epithermal region, a simple relationship derived in reference 2 may be used here:

$$p_{th} = \exp\left(\frac{-2\Sigma_{A,0.025}}{N^H \overline{\sigma}_S{}^H}\right)$$

An effective value of $\bar{\sigma}_s^H$ for the epithermal region is used and has the value of 34 barns for water at room temperature (see ref. 2). It is convenient to introduce the parameter K_{th}, which leads to

$$p_{th} = \exp\left(\frac{-2v\sigma_{F,0.025}}{R\,\bar{\sigma}_s^H K_{th}}\right) = \exp\left(\frac{-83.9}{K_{th}R}\right)$$

In figure 5, p_{th} is plotted against K_{th}. The preceding approximation is shown by the solid curve, while the value as calculated by numerical integration for four uranyl-fluoride - water solutions is shown by the circles. The same comparison is made in the following table:

R	p_{th}	
	Approximate	Numerical integration
24.4	0.187	0.211
52.9	.457	.443
99.5	.653	.628
221	.817	.795

Figure 6 was used to provide values of p_{th} for all solutions.

Fast Parameters

The fast-neutron slowing-down length L_f^2 was computed with the method of Marshak (ref. 22, eq. (A-3)) for water and solutions of uranyl fluoride of different concentrations. The results were averaged over the U-235 fission spectrum (ref. 23). Because the UO_2F_2 used in the criticality experiments was only 93.4 percent enriched in U-235, consideration was given to the scattering properties of the fluoride associated with U-234 and U-238. The results of this calculation gave $L_f^2 = 25.36$ square centimeters for pure water. This calculated value for pure water was adjusted to the experimental value of slowing-down length to thermal energies of 31.8 square centimeters (ref. 24). The values for the fluoride solutions were similarly adjusted by the same ratio. A curve of adjusted values of L_f^2 against $1/R$ is presented in figure 6. Also included in figure 6 is a curve of $\bar{\tau}_1$ and $\left(L_f^2 - \bar{\tau}_1\right)$. Values required for all fluoride solutions were read from the curve.

The material parameters used for each uranyl-fluoride solution are given in table I.

Geometric Buckling

The geometric buckling B^2 for a reactor of cylindrical geometry is given by

$$B^2 = \left(\frac{2.405}{r + \delta}\right)^2 + \left(\frac{\pi}{h + 2\delta}\right)^2$$

where r and h are reactor radius and height, respectively, in centimeters, and δ is either an extrapolation distance for a bare reactor or a reflector savings for a reflected reactor.

Since the extrapolation distance is given by $0.71\lambda_{TR}$, there arises the question of energy dependence of B^2. For the purpose of simplifying calculations, it was assumed that there was negligible energy dependence on the geometric buckling. However, the value of λ_{TR} or δ must be evaluated at neutron energies representative of where the bulk of leakage occurs. The scattering cross sections in the region of 1 Mev were chosen as representative of the fast leakage region. Since the scattering cross sections do not vary rapidly with energy in the neighborhood of 1 Mev, this assumption appears reasonable. An average $\overline{\Sigma}_{TR}$ is then evaluated as follows:

$$\overline{\Sigma}_{TR} = N^H\left[\overline{\sigma}^H_{TR} + \frac{1}{2}\overline{\sigma}^O_{TR} + \frac{1}{0.934}\left(\frac{2}{R}\overline{\sigma}^F_{TR} + \frac{2}{R}\overline{\sigma}^O_{TR} + \frac{1}{R}\overline{\sigma}^U_{TR}\right)\right]$$

where the average cross sections at about 1 Mev listed previously are used and cognizance is taken of the fact that the UO_2F_2 used in the solutions is only 93.4 percent enriched in uranium-235. Using the listed cross sections, the preceding relation becomes

$$\overline{\Sigma}_{TR(1\ Mev)} = N^H\left(3.175 + \frac{20.85}{R}\right)\times 10^{-24}$$

The extrapolation distance $\delta = 0.71/\overline{\Sigma}_{TR}$ is indicated to be a function of R and is listed in table I along with the other material parameters. It is noted that δ varies slowly with R.

The reactors of references 7 and 8 were enclosed in steel or aluminum containers 1/16 inch thick. If the shells are considered to be

thin reflectors, the savings can be approximated by use of the following relation (ref. 2):

$$\delta = \frac{\lambda_{TR,c}}{\lambda_{TR,r}} t$$

where t is the thickness in centimeters, and $\lambda_{TR,c}$ and $\lambda_{TR,r}$ are fast core and reflector transport mean free paths, respectively. From this relation, values of $\delta_{steel} = 0.22$ centimeter and $\delta_{Al} = 0.15$ centimeter are obtained. Inasmuch as relative absorptivities were not considered, these reflector savings were not included in computing K_{eff}.

The reflected reactors of references 7 and 8 were enclosed by varying thicknesses of water, with a minimum radial thickness of 11.43 centimeters. Two-group reflected spherical reactor calculations were made for four values of U-235 concentrations, namely $R = 24.4$, 43.9, 99.5, and 999. A table of calculated reflector savings against thickness for these four ratios follows:

t, cm	Reflector savings, δ, cm			
	$R = 24.4$	$R = 43.9$	$R = 99.5$	$R = 999$
5	4.95	4.65	4.50	4.30
10	7.20	6.55	6.18	5.85
30	7.75	7.00	6.60	6.25

The family of curves of reflector savings against reflector thickness is given in figure 7.

All the reflected reactors of reference 7 had a 6-inch reflector on top and a $4\frac{1}{2}$-inch reflector on bottom. The reactors of reference 8 had 6 inches of water. According to two-group theory, the saturated reflector savings for water reflectors on lean water-moderated cores should be approximately (see ref. 2)

$$\delta = \sqrt{L_f^2 + L_{th}^2} = \sqrt{31.8 + 7.66} = 6.28 \text{ cm}$$

which is in excellent agreement with the value obtained for $R = 999$ at $t = 30$ centimeters. The value of δ for reflected reactors obtained by Clark (ref. 12) is around 6 centimeters, which is in good agreement with

the present values. Bucklings for the reflected experimental assemblies were determined by the following formula:

$$B^2 = \left(\frac{2.405}{r + \delta_{S(\text{radial})}}\right)^2 + \left(\frac{\pi}{h + \delta_{S(\text{top})} + \delta_{S(\text{bottom})}}\right)^2$$

APPENDIX C

DETERMINATION OF EFFECT OF EXPERIMENTAL ERROR UPON REACTIVITY PREDICTIONS

The authors of reference 7 break down the experimental error into two types; a ±2-millimeter error in measuring the critical height, and a ±2-percent error in estimating the uranium concentration. An error in measuring the critical height would be more important for the flatter cores; an error in uranium concentration would be more important for the leaner, less concentrated cores.

Seven representative bare reactors of various height-diameter ratio were chosen, and the estimated experimental errors were introduced into a reactivity calculation to evaluate the increase in K_{eff}. The critical height was increased by 2 millimeters, which decreased the axial buckling. The uranium concentration was increased by 2 percent, which altered all the material parameters of reference 7. Results are shown in the following table:

Reactor[a]	R	Height/diameter	ΔK due to change in height, %	ΔK due to change in critical mass, %	Total ΔK, %
A-1	52.9	1.34	0.11	0.08	0.19
A-6	755	1.14	.06	.55	.61
S-1	43.9	1.27	.10	.12	.22
S-5	174	1.52	.08	.16	.24
S-15	119	.28	.71	.07	.78
S-17	329	.34	.54	.14	.68
S-19	755	.53	.25	.57	.82

[a]Arbitrary designation, A (aluminum), S (steel).

For the shortest reactor (height of 14.3 cm), the uncertainty in height produced an increase in reactivity of 0.71 percent. For the longer reactors, the change in K_{eff} was correspondingly less. The rich reactors showed little change in reactivity due to an error in U-235 concentration, while the leaner reactors showed as much as a 0.57-percent change in K_{eff}. It can be seen that the experimental error may account for as much as ±0.80-percent ΔK of the calculated value of K_{eff}.

REFERENCES

1. Bogart, Donald, and Valerino, Michael F.: The Sodium Hydroxide Reactor: Effect of Reactor Variables on Criticality and Fuel-Element Temperature Requirements for Subsonic and Supersonic Aircraft Nuclear Propulsion. NACA RM E52I19, 1952.

2. Bogart, Donald, and Soffer, Leonard: Criticality Survey of Hydroxides as Coolant Moderators for Aircraft Nuclear Reactors. NACA RM E53F30, 1953.

3. McCready, Robert R., Spooner, Robert B., and Valerino, Michael F.: Distribution of Fissionable Material in Thermal Reactors of Spherical Geometry for Uniform Power Generation. NACA RM E52C11, 1952.

4. Fox, Thomas A., and Bogart, Donald: Spatial Burnout in Water Reactors with Nonuniform Startup Distributions of Uranium and Boron. NACA RM E55C16, 1955.

5. McCready, Robert R.: Extrapolation Techniques Applied to Matrix Methods in Neutron Diffusion Problems. NACA TN 3511, 1955.

6. Bogart, D., and Valerino, M. F.: Some Epithermal Effects on Criticality Requirements of Water-Moderated Reactors. TID-2014, Reactor Sci. and Tech., vol. 4, no. 3, Sept. 1954, pp. 107-114.

7. Beck, C. K., Callihan, A. D., Morfitt, J. W., and Murray, R. L.: Critical Mass Studies, pt. III. K-343, Carbide and Carbon Chem. Corp., Apr. 19, 1949.

8. Blizard, E. P., ed.: Critical Experiments. Phys. Div., Semiannual Prog. Rep. for Period Ending Mar. 10, 1955. ORNL 1926, Oak Ridge Nat. Lab., Sept. 7, 1955.

9. Schuske, C. L., and Morfitt, J. W.: An Empirical Study of Some Critical Mass Data. Y-533, Carbide and Carbon Chem. Corp., Dec. 6, 1949.

10. Schuske, C. L., and Morfitt, J. W.: Empirical Studies of Some Critical Mass Data, pt. II. Y-829, Carbide and Carbon Chem. Co., Dec. 5, 1951.

11. Macklin, R. L.: Cylindrical Reactor Dimensions of the Water Tamped Enriched Uranyl Fluoride-Water System as a Function of Concentration. Rep. No. K-905, Carbide and Carbon Chem. Co., May 9, 1952.

12. Clark, H. K.: One-Group Analysis of Criticality Experiments. DP-59, E.I. du Pont de Nemours & Co., Nov. 1954.

13. Greuling, E.: Theory of Water-Tamped Water Boiler. LA-399, Los Alamos Sci. Lab., Univ. Calif., Sept. 27, 1945.

14. Greuling, E.: Graphical Method of Obtaining Critical Masses of Water-Tamped Water Boilers. LA-493, Los Alamos Sci. Lab., Univ. Calif., Apr. 5, 1946.

15. Mills, C. B.: The Small Hydrogen-Moderated Reactor. TID 2011, Reactor Sci. and Tech., vol. 3, no. 4, Dec. 1953, pp. 301-302.

16. Bell, George I.: A Simple Method of Calculating Critical Masses of Proton Moderated Assemblies. LA-1458, Los Alamos Sci. Lab., Univ. Calif., May 1953.

17. Bendt, Philip J.: Hydrogen Slowing-Down Method for Criticality Calculations. LA-1581, Los Alamos Sci. Lab., Univ. Calif., Sept. 1953.

18. Danzker, Milton: An Interpretation of Data on Enriched Hydrogenous Thermal Reactors. WAPD-26, Atomic Power Div., Westinghouse Electric Corp., Jan. 9, 1951.

19. Neutron Cross Section Advisory Group of Atomic Energy Commission: AECU 2040, May 15, 1952. (Available from Office Tech. Services, Dept. Commerce.)

20. Anon.: Neutron Cross Sections: A Compilation of the AEC Neutron Section Advisory Group. BNL-170, Brookhaven Nat. Lab., Upton (N.Y), May 15, 1952.

21. Glasstone, Samuel, and Edlund, Milton C.: The Elements of Nuclear Reactor Theory. D. Van Nostrand Co., Inc., 1952.

22. Marshak, Robert E.: Theory of the Slowing Down of Neutrons by Elastic Collision with Atomic Nuclei. Rev. Modern Phys., vol. 19, no. 3, July 1947, pp. 185-238.

23. Watt, B. E.: Energy Spectrum of Neutrons from Thermal Fission of U^{235}. Phys. Rev., vol. 87, no. 6, Sept. 15, 1952, pp. 1037-1041.

24. Hill, J. E., Roberts, L. D., and Fitch, T. E.: The Slowing Down Distribution from a Source of Fission Neutrons in Light Water. AECD-3392, Oak Ridge Nat. Lab., Dec. 10, 1948.

TABLE I. - MATERIAL PARAMETERS

R	K_{th}	$\bar{K}_1$	p_{th}	L_f^2, cm^2	$(L_f^2 - \bar{\tau}_1)$, cm^2	L_{th}^2, cm^2	δ, cm
24.4	2.052	1.800	0.187	36.81	35.25	0.132	3.24
26.2	2.051	1.799	.210	35.95	34.50	.136	3.22
26.9	2.050	1.798	.218	35.64	34.28	.149	3.15
29.9	2.047	1.796	.254	34.73	33.49	.150	3.21
31.6	2.045	1.795	.273	34.31	33.19	.153	3.21
43.9	2.033	1.789	.391	32.97	32.11	.193	3.21
52.9	2.024	1.785	.457	32.58	31.84	.223	3.22
56.7	2.021	1.784	.481	32.47	31.79	.236	3.23
58.8	2.019	1.783	.493	32.42	31.75	.243	3.23
61.1	2.017	1.782	.506	32.39	31.72	.250	3.23
62.7	2.015	1.780	.515	32.34	31.71	.257	3.23
71.5	2.007	1.776	.557	32.31	31.65	.308	3.24
73.4	2.005	1.775	.566	32.20	31.61	.315	3.25
74.0	2.005	1.775	.568	32.20	31.61	.317	3.25
75.3	2.003	1.772	.573	32.20	31.61	.322	3.25
86.4	1.993	1.772	.614	32.10	31.60	.337	3.26
99.5	1.980	1.762	.653	32.03	31.58	.382	3.27
119	1.962	1.753	.698	31.98	31.57	.446	3.27
123.2	1.959	1.751	.707	31.98	31.57	.460	3.28
169	1.918	1.726	.772	31.89	31.58	.607	3.29
174	1.914	1.724	.778	31.88	31.58	.623	3.29
192	1.898	1.715	.795	31.86	31.59	.679	3.29
221	1.874	1.700	.817	31.85	31.59	.767	3.30
226	1.870	1.697	.820	31.83	31.59	.781	3.30
290	1.819	1.665	.853	31.82	31.60	.966	3.30
320	1.796	1.650	.864	31.82	31.60	1.049	3.30
329	1.789	1.646	.867	31.81	31.60	1.075	3.31
499	1.669	1.559	.905	31.80	31.61	1.509	3.31
755	1.516	1.444	.930	31.79	31.61	2.065	3.32
999	1.395	1.348	.942	31.79	31.63	2.511	3.32
∞	0	0	.981	31.79	31.65	7.649	3.35

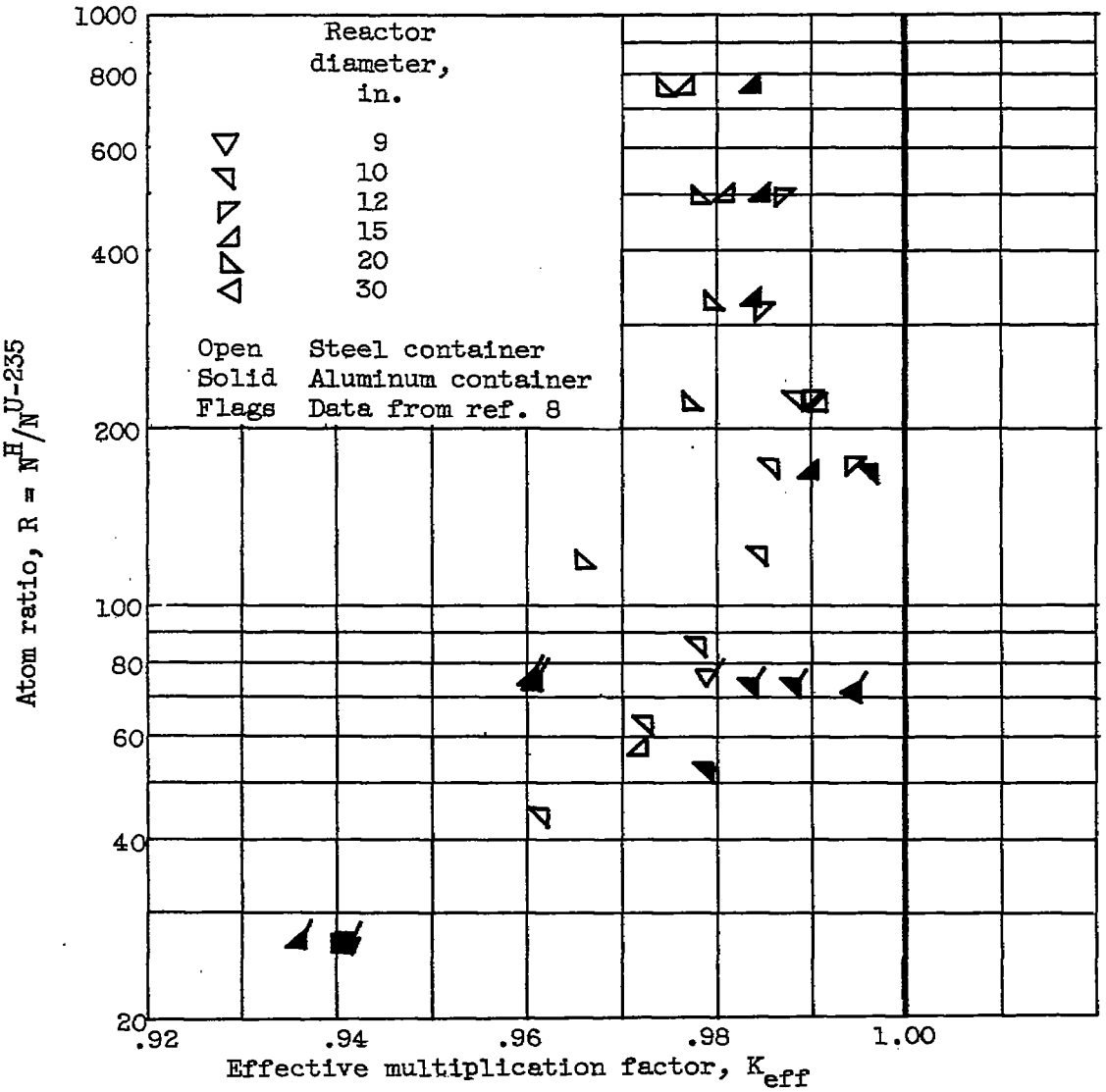

Figure 1. - Effective multiplication factor for bare uranyl-flouride - water cylindrical critical assemblies of references 7 and 8.

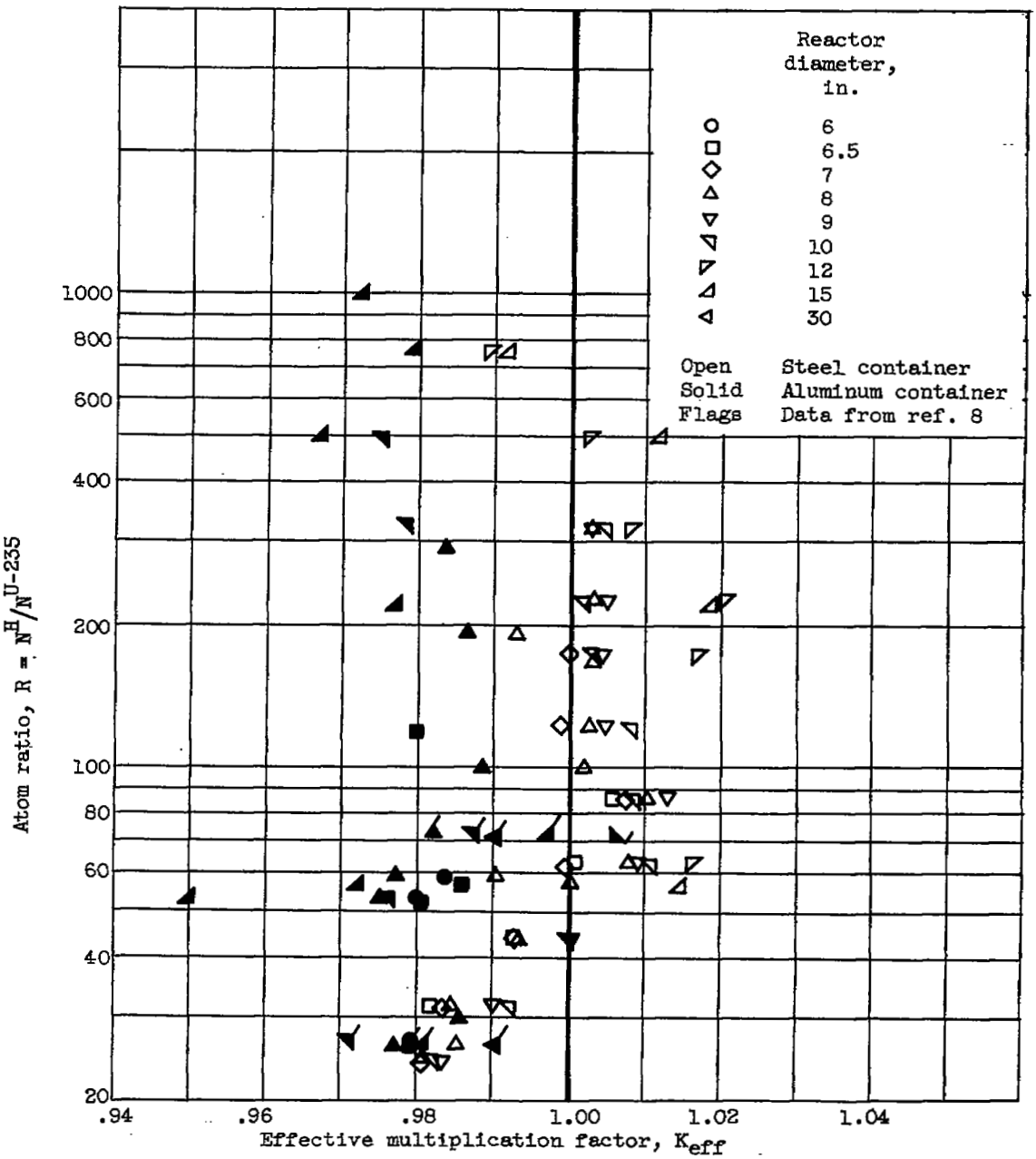

Figure 2. - Effective multiplication factor for reflected uranyl-flouride - water cylindrical critical assemblies of references 7 and 8.

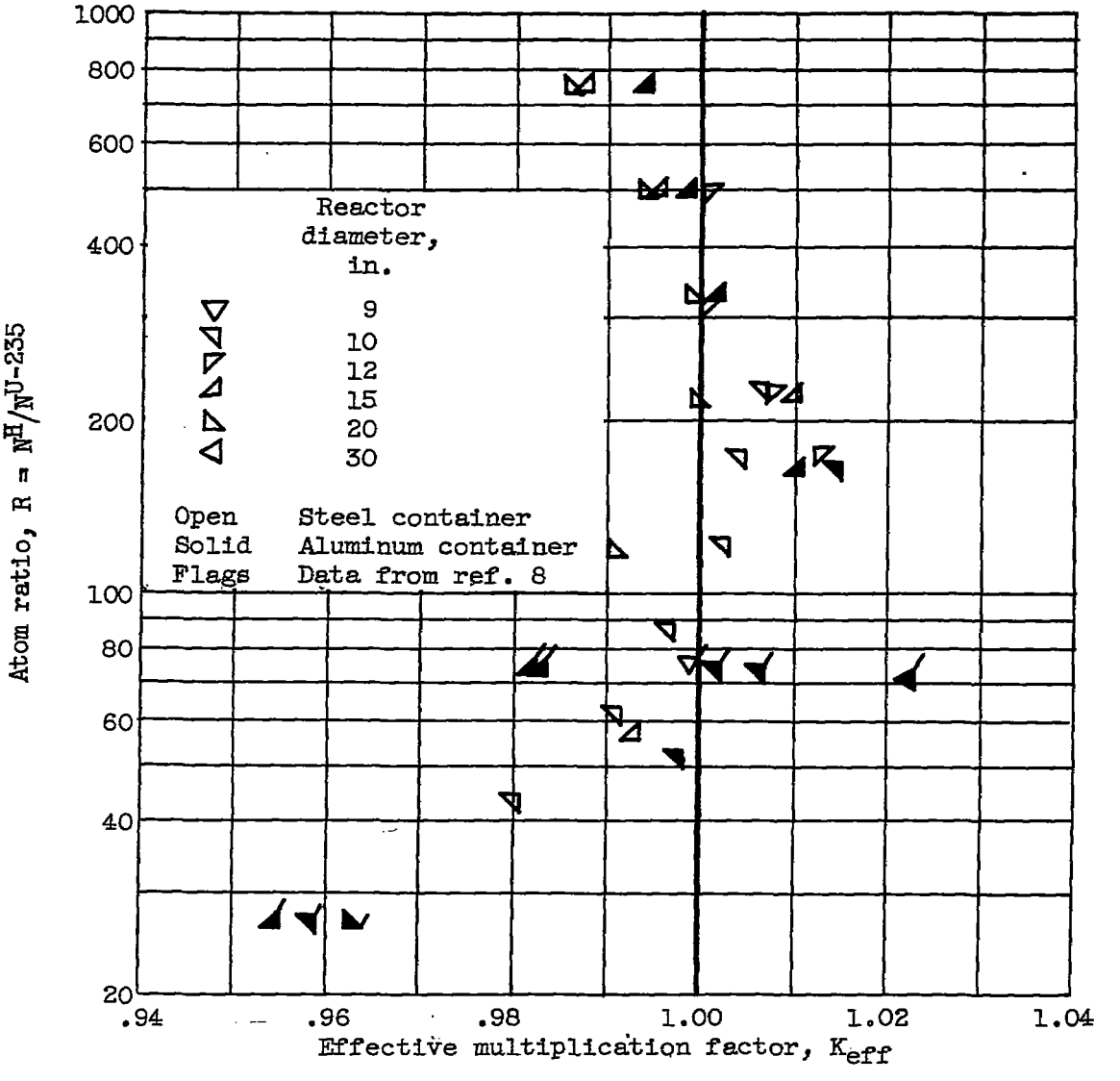

Figure 3. - Effect of 10-percent increase of extrapolation distance on effective multiplication factor for bare uranyl-flouride - water cylindrical critical assemblies of references 7 and 8.

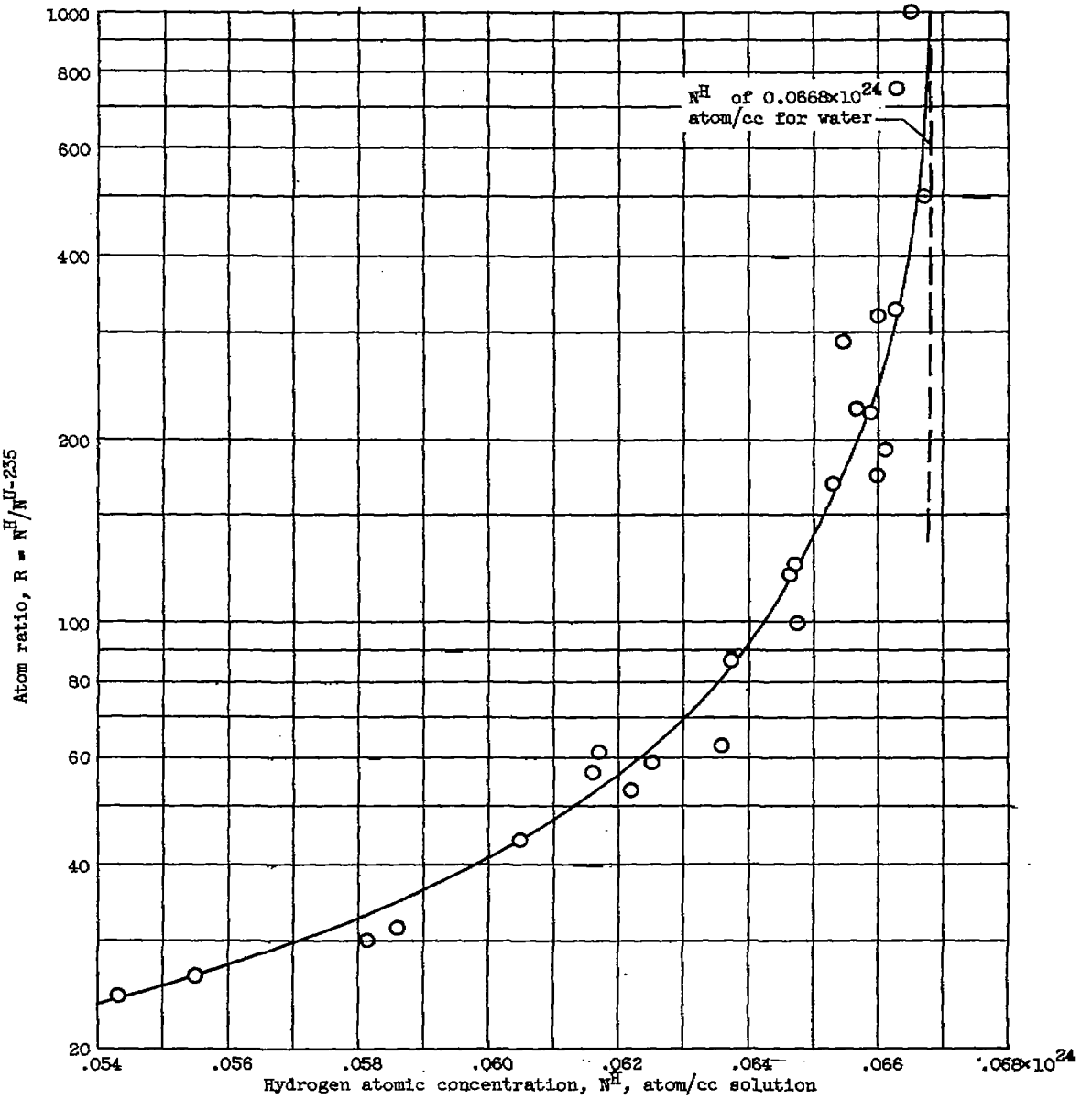

Figure 4. - Uranium atomic concentration as function of hydrogen atomic concentration for various uranyl-flouride - water solutions at room temperature, calculated from experimental data of reference 7.

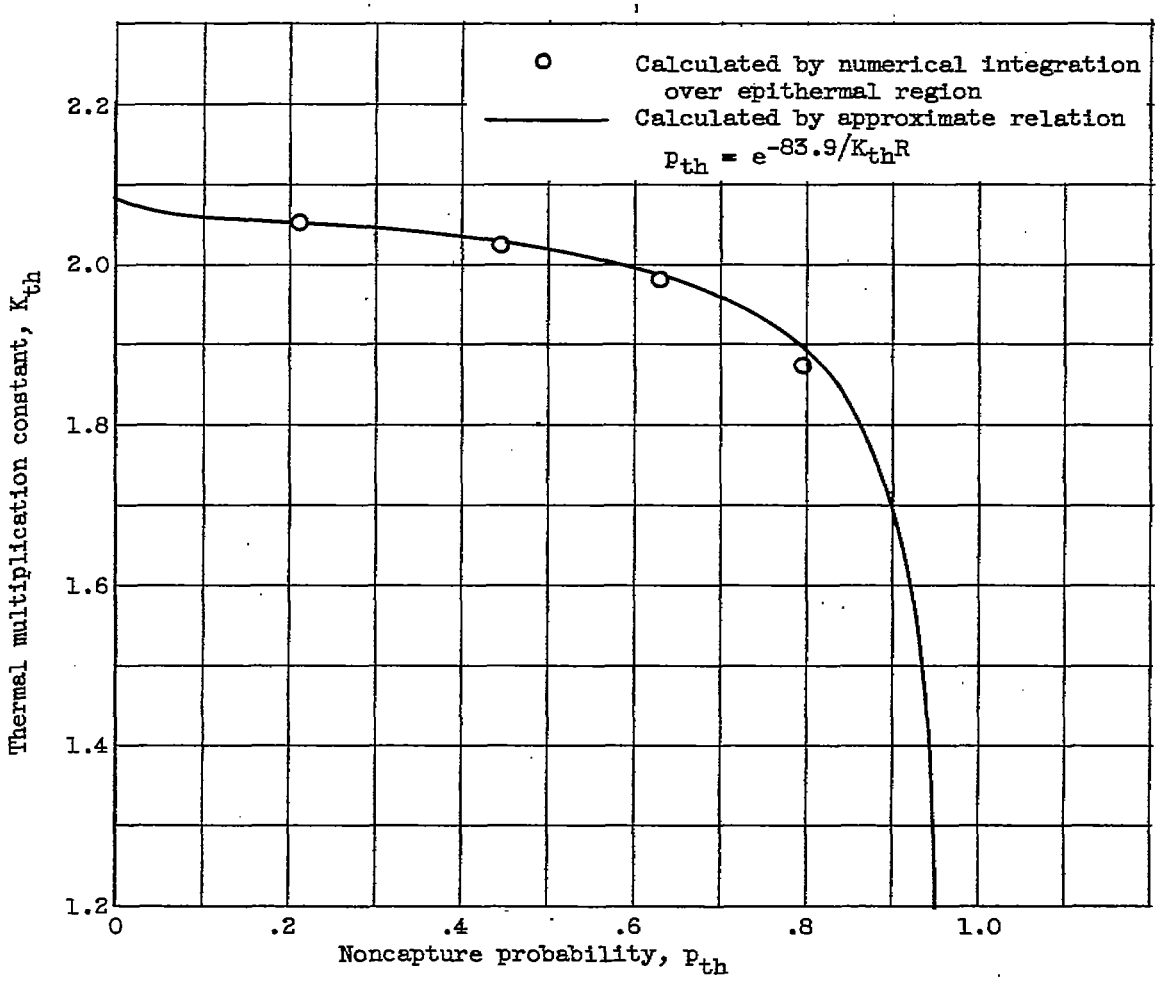

Figure 5. - Noncapture probability for uranyl-flouride - water solutions at room temperature.

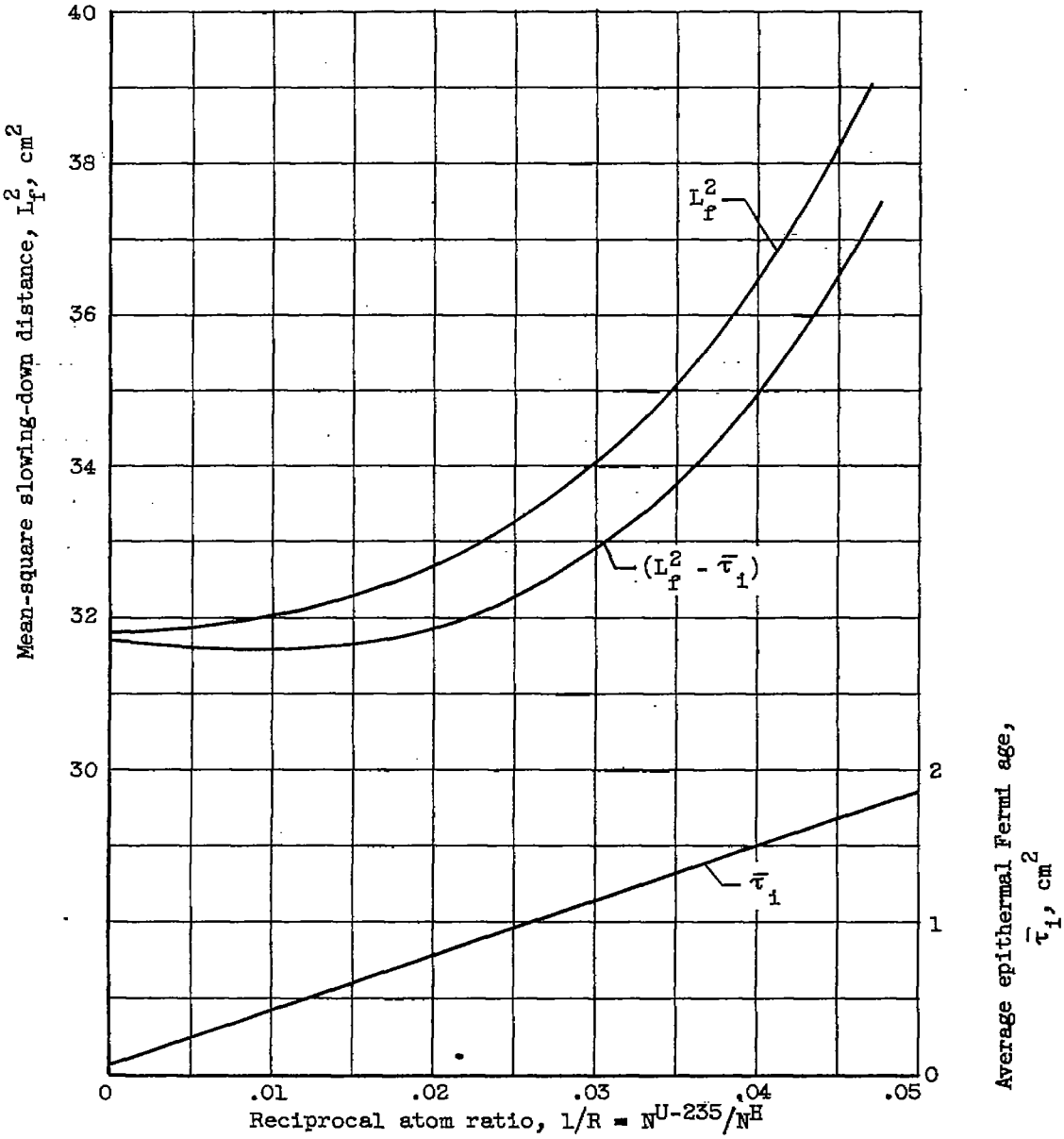

Figure 6. - Mean-square slowing-down distance for uranyl-flouride - water solutions at room temperature.

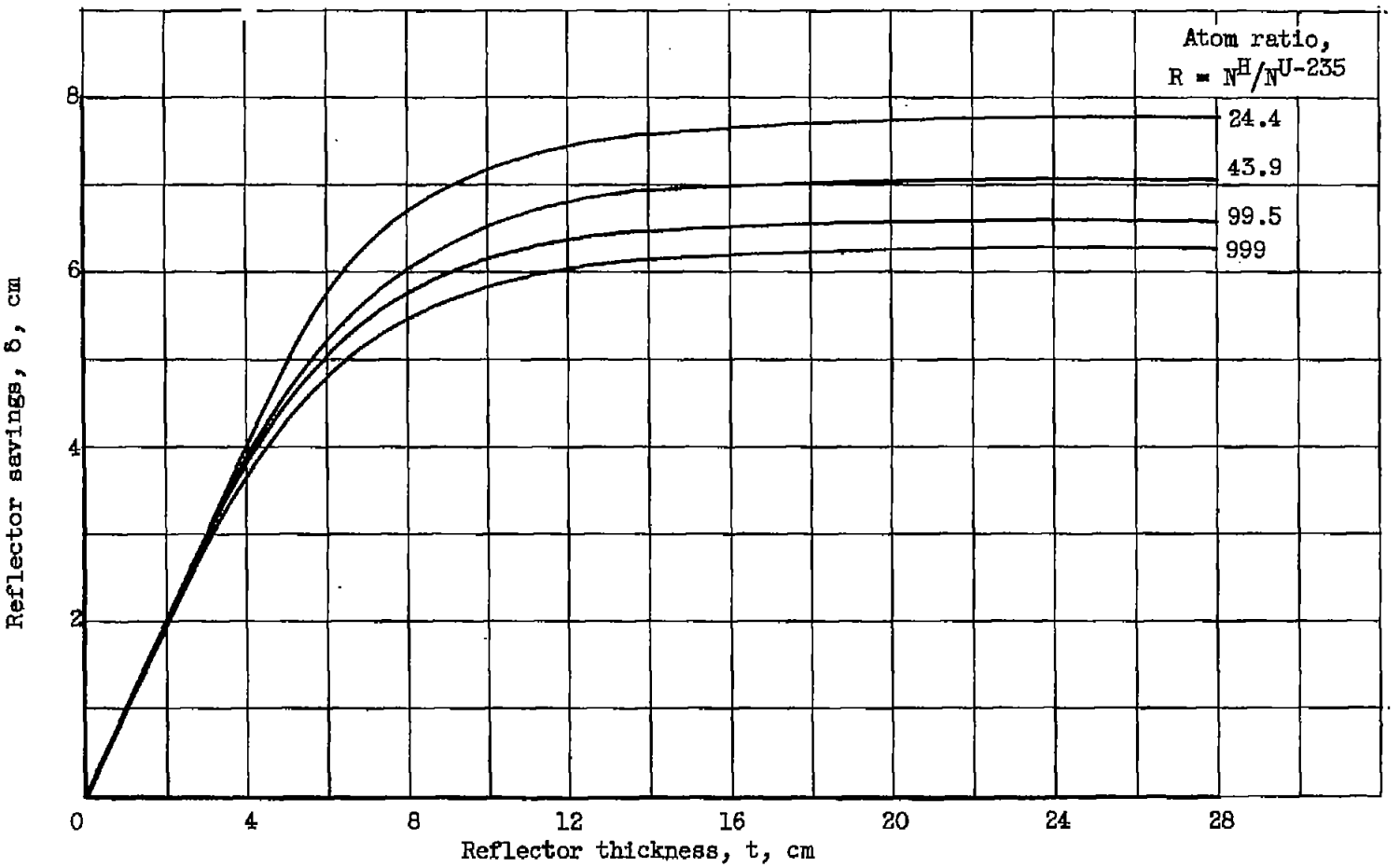

Figure 7. - Reflector savings due to water reflector for uranyl-flouride - water solutions at room temperature, calculated by two-group theory.